A Letters Journal Exploring
the Frontiers of Physics

January 2020

EPL, **129** (2020) 15003
doi: 10.1209/0295-5075/129/15003

www.epljournal.org

Generation of compact plasma objects in plasma focus discharge

V. I. Krauz[1(a)], M. Paduch[2], K. Tomaszewski[3], K. N. Mitrofanov[4], A. M. Kharrasov[1], A. Szymaszek[2] and E. Zielinska[2]

[1] *National Research Centre Kurchatov Institute - Akademika Kurchatova pl., 1, 123182 Moscow, Russia*
[2] *Institute of Plasma Physics and Laser Microfusion - Hery street 23, 01-497 Warsaw, Poland*
[3] *ACS Ltd - Hery street 23, 01-497 Warsaw, Poland*
[4] *Troitsk Institute for Innovation and Fusion Research - Pushkovyh street, 12, 108840 Moscow, Troitsk, Russia*

received 12 September 2019; accepted in final form 21 January 2020
published online 13 February 2020

PACS 52.59.Hq – Dense plasma focus
PACS 52.30.-q – Plasma dynamics and flow
PACS 52.72.+v – Laboratory studies of space- and astrophysical-plasma processes

Abstract – This paper provides the results of studies of plasma flows generated in the plasma focus facility PF-1000U. Regimes are found, involving the formation of compact plasma objects propagating in the variable-density background environment to the distances exceeding the initial crosswise dimensions of these objects by dozens of times. It is shown that the flow spreads with its proper captured toroidal magnetic field. The plasma flow front structure is studied. The conclusions about the role of radiation cooling and magnetic confinement in the collimation and stability of outflows are drawn. The results obtained in this work can be used to analyze the existing and build new models describing the collimation and stability of non-relativistic outflows of young stellar objects.

Introduction. – One of the interesting recently developed trends is the laboratory modeling of jet ejections of young stellar objects (YSO) [1,2]. There are several well-known papers about modeling these ejections using fast Z-pinches [3], powerful lasers [4], plasma guns [5]. The devices used to simulate astrophysical jets are not limited to those listed above. For example, good prospects for X-pinches were shown [6–8]. Plasma focus (PF) facilities with their pinch-effect operation principle are widely known as intensive sources of plasma flows extensively used in various practical applications [9–12]. One of the interesting applications of PF systems is the modeling of various astrophysical and cosmic phenomena (see, for example, [13–15]). Lately, flows generated in PF have also been used to model astrophysical jets [16–20]. As shown in [21–24], PF facilities comply with the basic similarity laws necessary for modeling astrophysical jets, which makes it legitimate to use these devices in such experiments. It is noteworthy that plasma jets, applicable for laboratory modeling, can be obtained not only at large facilities, but also at significantly smaller facilities operating at discharge energy of only a few tens of joules [18].

One of the strengths of the modeling pattern based on PF systems is the opportunity to study the behavior of the parameters of plasma flows spreading at large distances. As shown in earlier papers, the distances at which flows generated in the plasma focus discharge in the pinching phase may spread exceed their initial crosswise dimensions by two orders [17,23]. A distinct feature of this experimental setup is the fact that the flows spread in a gas-filled chamber, which allows studying the influence of the contrast (the flow-to-environment density ratio) on the flow dynamics. The range of experimental conditions can be considerably expanded by creating profiled distributions of gas through gas puffing. That said, the initial gas distribution will be determined by the region of additional injection. For example, in the experiments on the KPF-4 Phoenix facility conducted at the Sukhum Physical Technical Institute the gas was injected into region of the discharge system insulator, which allowed creating a low-density distribution in the plasma flow propagation area [20,25]. The PF-1000U facility operated at the Institute of Plasma Physics and Laser Microfusion in Warsaw uses the axial injection into the pinch formation area [20,21]. The previous experiments with the injection of neon and deuterium brought to light the formation of

(a) E-mail: krauz_vi@nrcki.ru

complex spatial structures [26] in the pinching area. This work aims to study the influence of axial gas puff on the plasma flow parameters.

Experimental setup. – The experiments were conducted on the PF-1000U facility ($W_{\max} \approx 1\,\mathrm{MJ}$, $V_{\max} = 40\,\mathrm{kV}$) made as a PF with a Mather-geometry electrode system [27] (fig. 1). The facility's inner electrode (anode) is a thin-wall copper cylinder of 230 mm in diameter and 460 mm in length; the outer electrode (cathode) consists of twelve 80 mm thin-wall stainless steel tubes evenly distributed around a circumference with a radius of 200 mm. A ceramic insulator of 230 mm in diameter and 85 mm in length separates the anode from the cathode. The electrode system is placed in a quite large vacuum chamber of 140 cm in diameter and 250 cm in length, which allowed studying the dynamics of flow propagation at fairly large distances.

After preliminary pumping the chamber was filled at $P = 0.9$ Torr with deuterium or a mix of deuterium and helium added for diagnostic purposes. After the voltage from the capacitor bank is applied to the electrodes of the discharge system, a plasma current-carrying sheath (PCS) forms in the insulator area and, exposed to Ampère forces, moves to the anode butt end, and contracts closer to the axis, which causes the formation of a pinch. The latter process is attended by the dissipation of the magnetic energy accumulated in the circuit and the occurrence of a dip in the discharge current derivative. The successive positions of the PCS and the pinch formation area are also shown in fig. 1. The pinch is a source of various emissions, including plasma flows spreading at supersonic speeds along the system axis and being the main object of our research.

The anode has an axial channel with a diameter of 50 mm, inside of which there is an annular nozzle of a quick-acting valve for gas puffing with an external diameter of 40 mm and a width of 6 mm. In the experiments being described the gas (D_2, He, Ne, or their mixes) was injected in the chamber around two ms before the discharge was initiated through the axial passage in the central electrode. The gas pressure under the valve was 1.2–1.5 atm. The study did not involve any gas density distribution measurements; according to estimates, however, by the time the discharge is initiated the injected gas manages to spread at no more than 15 to 20 cm. Since the gas escapes into the vacuum with hydrodynamic times, the gas distribution during a discharge of several tens of microseconds can be considered constant. Thus, the contoured initial gas distribution was created with an increased density in the area of pinch formation and plasma flow generation. Then the flow continues to spread into the low-density area, which corresponds to known astrophysical models [28].

The main tool used to study the shape of the plasma flow was an HS-1F-VISc frame camera with an exposure of 3 ns. The field of view of the optic camera was 20.6 cm,

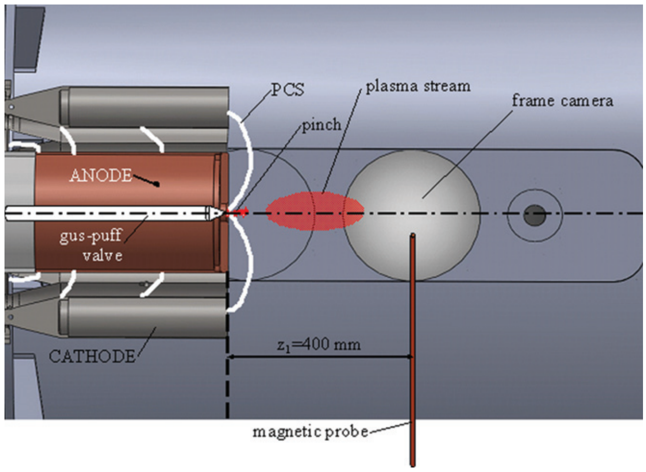

Fig. 1: Experimental setup.

whereas the distance between the frame center and the anode surface was 41.5 cm.

An absolutely gaged magnetic probe was positioned in the camera's field of view 40 cm away from the anode butt end. The sensing element of the probe consisted of three 5×3 mm five-turn coils tuned to register the $B\varphi$ field. The distance between the centers of the probe coils was 15 mm, which allowed us to evaluate the kind of radial distribution of the magnetic field captured by the flow. The calibration was performed in the homogeneous field of a Helmholtz coil relative to the reference loop with a known area.

The pinching process was registered using a four-frame HS-4F-SXRC X-ray camera with an exposure range of no more than 1.8 ns and delays of 16 to 35 ns between shots. Each frame of the camera had a 90×63 mm field of view, and the spatial resolution per object was at least 1 line mm^{-1} (or $0.0934\,\mathrm{mm\,pxl}^{-1}$ on digital image). The spectral sensitivity range varied from 10 eV to 6 keV.

The flow optic emission was also registered using optic collimators that transmitted the radiation from the narrow range (∼1 cm on the camera axis) along the chamber diameter to the photo cathode of the photo multiplier. The experiments in question were conducted using two collimators oriented at the region of 35 and 37 cm along the axis relative to the anode butt end.

Thus it was possible to control the instant, when the flow entered the observed area, and use the time shift between signals from the collimators to estimate the flow propagation velocity in that section. Considering the short distance between the points of observation, we can actually talk about the instantaneous flow velocity in this region.

The discharge current derivative was registered using a loop sensor. The dip in the discharge current derivative was taken for a conventional zero. Thus the current derivative signal was used for synchronizing all the diagnostics. The full discharge current was measured using

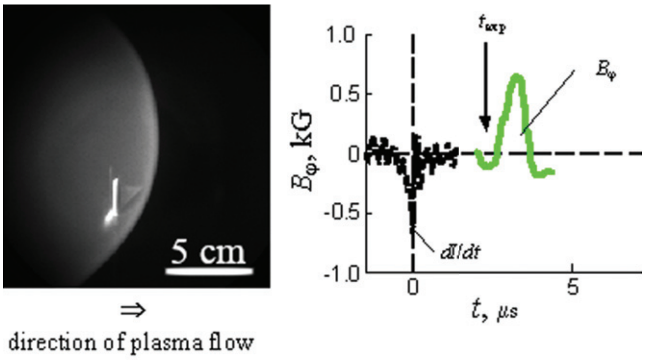

(a) (b)

Fig. 2: (a) Picture of a plasma flow at the stationary filling of deuterium and (b) the time dependencies of the discharge current derivative and magnetic field registered by the probe installed 40 cm away from the anode butt end and a radius of 5 cm relative to the chamber axis. The arrow in fig. 2(b) indicates the optic frame camera's exposure instant. The flow moves from left to right.

a Rogowski coil. The experiments were conducted at a discharge energy of 170 kJ ($U_0 = 16$ kV) and a discharge current of 1.5–1.8 MA.

Experimental results. – The experiments revealed that the flow structure was significantly affected by the condition in which the chamber was filled with the working gas. The picture of the flow generated, when the chamber was filled in stationary mode with pure deuterium, is shown in fig. 2. Only the shockwave (SW) front is seen in the picture but there are no visible structures associated with the flow. At the same time, fig. 2 shows that the magnetic probe located already beyond the SW front indicates the existence of a magnetic field building up over time. As shown by analyzing the data obtained in discharges with various delays of the shot exposure relative to the dip in the current derivative instant, the magnetic field is not registered right until the shock comes. The field registered in the SW front may have different signs. The field increases in strength as the probe plunges into the flow. At the same time, a signal from the magnetic probe has a finite length of $\sim 1\,\mu$s for a given discharge: at a propagation velocity of $\sim 10^7\,\mathrm{cm\,s^{-1}}$ this corresponds to finite longitudinal sizes of structures with a magnetic field of ~ 10 cm. It is thus possible to state that a shockwave is followed by some plasma formation with a longitudinal current, unresolvable by optical diagnostics.

That said, the kind of radial distribution of the azimuthal magnetic field indicates that the current is concentrated mainly in the pre-axial zone. The negative field value in the flow front may have to do with the inhomogeneous spreading of closing reverse current.

A similar scenario is observed when the chamber is filled with deuterium with 10% of helium as an additive. However, if to additionally inject deuterium or helium through the valve into the pre-axial region of the chamber pre-filled

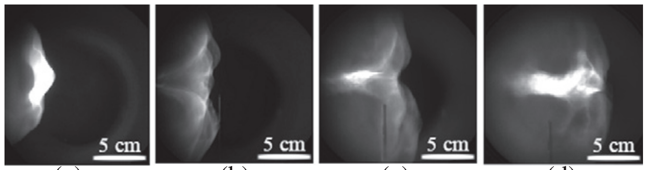

(a) (b) (c) (d)

Fig. 3: Pictures of the plasma flow 41.5 cm away from the anode end upon the pulse injection of (a) deuterium, ((b) and (c)) neon, and (d) deuterium-neon mix. The flow moves from left to right.

with deuterium, the situation will be radically different (fig. 3(a)). In this case it is seen that glowing structures appear in the SW front. Moreover, the front's more complex structure manifests. This is even more evident in the case of a pulse injection of pure neon (figs. 3(b) and 3(c)) or the deuterium-neon mix (fig. 3(d)). It is an amazing fact that structures with characteristic dimensions of about 1 cm are observed at a distance of more than 40 cm away from the anode butt end. If to suppose that a plasma flow forms in the pinching phase, this will actually mean that the formed plasma blob remains compact when spreading along the axis at distances of two orders in excess of its initial crosswise dimensions.

The results shown in fig. 4 are obtained in one discharge at the stationary filling of the chamber with deuterium at 0.9 Torr and the pulse injection of neon and serve to exemplify the formation and propagation of plasmoids. In the final discharge phase the pinch with a discharge current of about 1 MA is subject to strong instabilities. The development of instabilities $m = 0$ may cause an interruption of current, reconnection of magnetic field lines, and formation of a plasmoid with a captured magnetic flux. The formation of such structures, including in gas-puff modes, using laser interferometry and magnetic probes, was shown earlier in [29–32]. Affected by the magnetic field gradient, this plasmoid is pushed out along the axis. An example of formation of this plasmoid is shown in figs. 4(a), (c). Then the formed plasmoid spreads along the axis of the facility chamber. The picture of a flow in the visible range with a shot exposure of 3 ns, made about 30 to 40 cm away from the area of generation is shown in fig. 4(b). It is seen that even at such a distance the glowing core of ~ 1 cm in size continues to exist. Moreover, the track of this core along the chamber is well visible on the time-integral picture made with a digital camera (figs. 4(e) and 5(a)).

Unlike the discharge at the stationary filling with deuterium without pulsed injection (fig. 5(b)), the trace from the flow core is also observed at longer distances. That said, the track has an almost constant crosswise size but the spectrum of radiation varies from blue characteristic of Ne II to red characteristics for excited neutral Ne I. Since there must be no neon at large distances at the time of discharge with gas puff, first of all, the latter circumstance

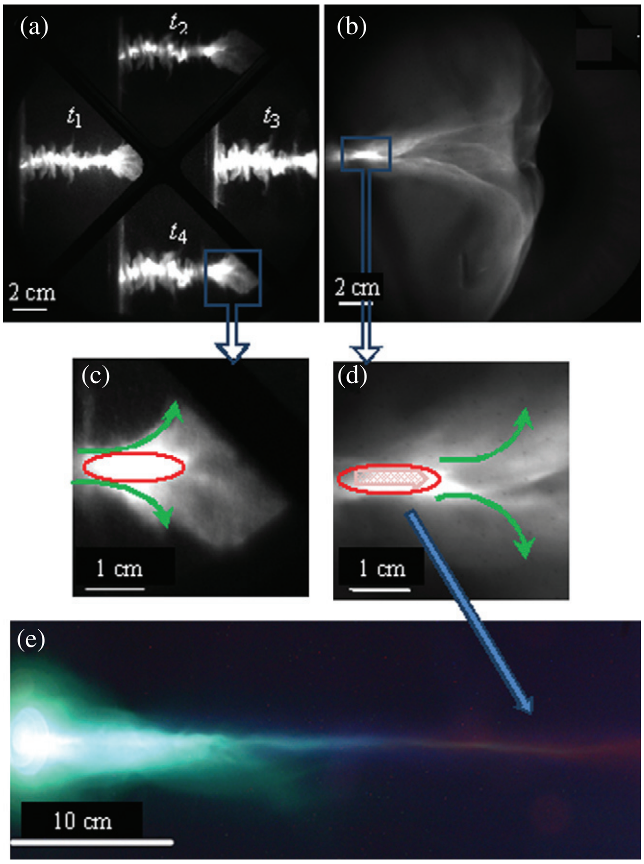

Fig. 4: (a) Consecutive pictures of the pinching region in the soft X-ray range, with the delay between the frames of 20 ± 5 ns, and (b) in the scaled up region of plasma flow formation; (c) picture of the plasma flow in the visible spectrum 40 cm away from the anode plane and (d) its scaled up central part; (e) time-integral picture of the plasma flow in the visible spectrum. The arrows on (c) and (d) indicate the direction of axial (red) and reverse (green) currents. The blue arrow on (e) indicates the place of flow core which is visible on (d).

indicates that the injected gas is involved in the carryover with the plasma flow and that the flow ions gradually cool down and recombine with a growing distance from the anode. Obviously, the availability of neon characterized by significant radiation losses is necessary for collimating the flow core. Unfortunately, we never achieved good-pinching regimes in the stationary neon filling experiments without gas puffing. Nonetheless, according to fig. 5(c), the compact core retaining its crosswise dimensions at large distances forms at stationary neon filling. It also bears mentioning the red luminosity spectrum of background gas, typical, as previously noted, of excited atom Ne I.

As the flow spreads, its parts with various luminosity successively pass by the optic collimator detecting the emission from the area 37 cm away from the anode. Actually, this means that the collimator scans the object luminance intensity. If the object motion velocity is known, the result of scanning the object's picture made using an optic frame camera can be juxtaposed with a certain degree of

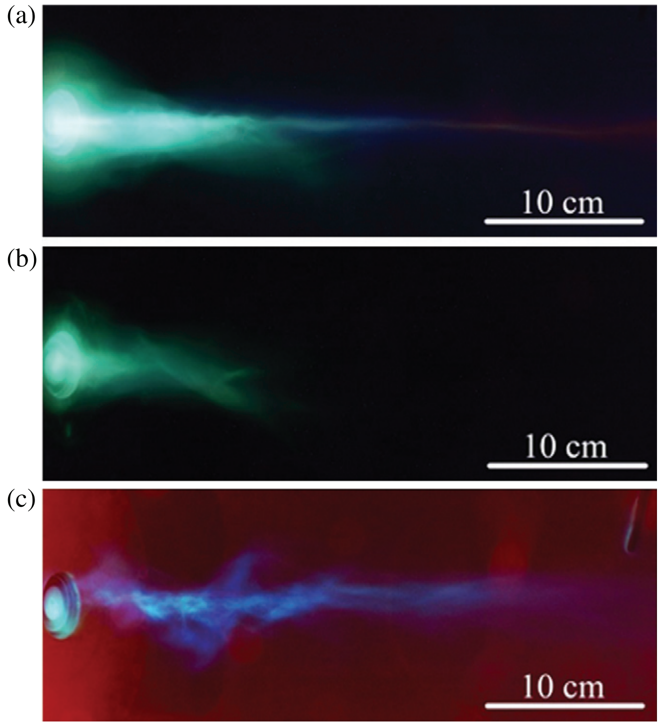

Fig. 5: Time-integral pictures of the plasma flow spreading in the visible spectrum. The flow spreads from left to right: (a) stationary filling of D_2 + gas-puff of Ne; (b) stationary filling of D_2 and (c) stationary filling of Ne.

accuracy against the shape of the signal from the collimator as done in fig. 6. The curves in this figure are derived on the assumption that the flow moves along the facility axis at velocity of $4.5\times10^6\,\mathrm{m\,s^{-1}}$ which is close to the velocity of $5.8\times10^6\,\mathrm{m\,s^{-1}}$ measured by the delay of signals from the light collimators when the flow passed the section between 35 and 37 cm. Some discrepancy in the velocity values may stem from the different detection regions of the optic camera and the collimator, deceleration of the flow spreading along the axis [29], and measuring inaccuracy.

Discussion and conclusions. – As already noted above, a glowing core and a funnel-shaped plasma flow front are observed at the pulsed injection of gas (figs. 4 and 6(b)). It follows from fig. 6 that the magnetic probe signal originates after the flow front passes the position of the magnetic probe, whereas the instant of the rapid buildup of the peak magnetic field value followed by its long-time existence closely corresponds to the instant when the probe is passed by the plasma flow core.

This behavior of the magnetic field agrees with the model formulated in [20,23,30,31]. In this model the plasma flow is a dense core in which the axial current flows creating a holding toroidal magnetic field (fig. 6(c)).

When this core spreads in background plasma, a shockwave is generated, to which some part of the mass outflows [24] that forms the environment for closing return currents; what is more, these currents may spread not

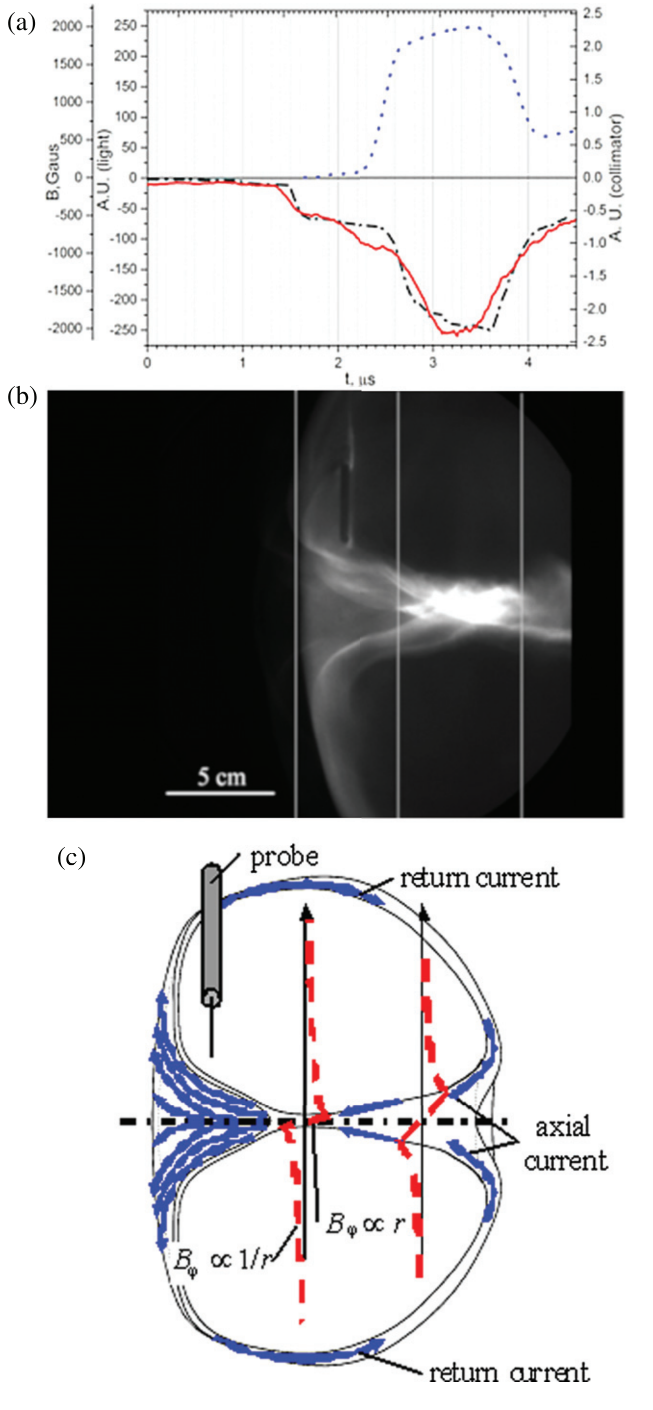

Fig. 6: (a) Signals from the magnetic probe (dashed line), light collimator (solid line) and result of the brightness scanning of the frame image of the flow (dot-dashed line) represented in panel (b) (the flow moves from right to left); (c) distribution pattern of the current in the flow.

homogeneously but as separate current channels. If there is some strongly emitting substance in the case of pulsed injection, these currents also manifest well against the weakly emitting deuterium. The latter circumstance tells on signals from the magnetic probe because they heavily depend on the position of the probe relative to the current channels.

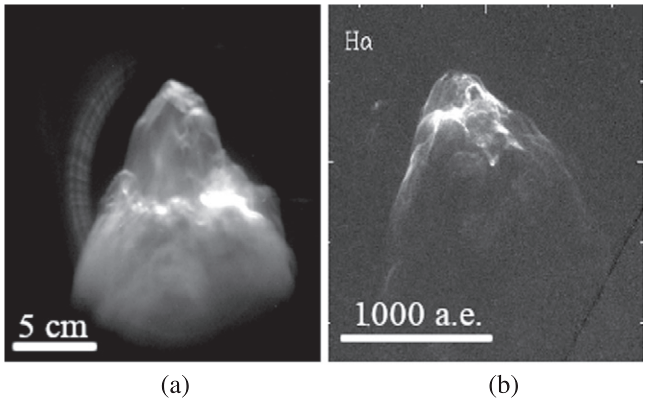

Fig. 7: Images of the head part of the flows, (a) made on PF-1000U in case of discharge in neon and (b) of the actual jet outflow observed in object HH34 [32].

Thus the existence of regions with elemental composition different from that in background gas allows us to better understand the flow structure. Because there are no such regions in case of discharges in pure deuterium, only the shockwave front is visible. A similar situation is observed in the case of discharges in pure neon. That said, the flow contour becomes conical, which is yet another indicator of the importance of radiation cooling. It should be noted that in this case the flow shape closely corresponds to the shape of real astrophysical jets (fig. 7).

As was shown, the development of instabilities $m = 0$ results in the reconnection of magnetic field lines, and formation of plasmoids with a captured magnetic flux. The formation of such structures, including in gas-puff modes, was shown earlier in [33–36] using laser interferometry and magnetic probes. In these papers conclusion was made about the influence of these processes on non-thermal acceleration of fast electrons and ions and production of hard X-rays and fusion neutrons. Undoubtedly, these processes play no less important role in the formation and acceleration of the compact and stable objects observed at significant distances from the pinch.

This study did not involve measuring the parameters of plasma in the early flow formation phase. However, assuming that the flow core forms upon the disintegration of the pinch which is in Bennett's equilibrium due to the development of MHD instabilities (fig. 4(a)), it would be logical to suppose that flow plasma and the pinch plasma have similar parameters. The neon pinch temperature is known to reach several hundred eV [37]. Neon plasma rapidly cools down due to high radiation losses. If the cooling rate exceeds the dissipation speed of the captured current and, respectively, the holding toroidal magnetic field, the central core contracts (collimates), which is seen in the comparison of the cross-dimensions of the bunches in figs. 4(a) and 4(b). It is thus seen that radiation cooling and magnetic confinement play a major role in the flow collimation and stability. One of the main tasks of further research will be to study in detail the distribution dynamics of the magnetic field in a plasma bunch spreading in ambient gas.

Thus, the used approach allowed to study in detail the structure of the plasma flow generated in the plasma-focus discharge. For the first time, plasmoids preserving their compactness when propagating in a background medium were found. As is known [38], one of the most interesting properties of astrophysical jets is their small divergence. The length of the jets of YSO is 0.01–2 pc, while the opening angle is only 5–10°. The results obtained in this work can be used to analyze the existing and build new models describing the collimation and stability of non-relativistic outflows of YSO.

* * *

The reported study was funded by Russian Foundation for Basic Research, project 18-29-21006_mk and by the Research Program under Grant IAEA Nos. 23071, 23225 as well by the Polish Ministry of Science and Higher Education within a framework of the international co-financed projects.

REFERENCES

[1] Ryutov D. D. and Remington B. A., *Plasma Phys. Control. Fusion*, **44** (2002) B407.
[2] Remington B. A., Drake R. P. and Ryutov D. D., *Rev. Mod. Phys.*, **78** (2006) 75.
[3] Lebedev S. V., Frank A. and Ryutov D. D., *Rev. Mod. Phys.*, **91** (2019) 025002.
[4] Albertazzi B., Ciardi A., Nakatsutsumi M. *et al.*, *Science*, **346** (2014) 325.
[5] Gunsu S. Yu. and Bellan P. M., *Phys. Plasmas*, **17** (2010) 062108.
[6] Beg F. N., Ciardi A., Ross I., Zhu Y., Dangor A. E. and Krushelnick K., *IEEE Trans. Plasma Sci.*, **34** (2006) 2325.
[7] Haas D. M., Bott S. C., Kim J. *et al.*, *Astrophys. Space Sci.*, **336** (2011) 33.
[8] Pavez C., Sepúlveda A., Cabrini N. *et al.*, *IEEE Trans. Plasma Sci.*, **46** (2018) 3829.
[9] Rawat R. S., *Nanosci. Nanotechnol. Lett.*, **4** (2012) 251.
[10] Borovitskaya I. V., Bondarenko G. G., Gaidar A. I. *et al.*, *Russ. Metall.*, **2** (2018) 266.
[11] Sadowski M. J., Gribkov V. A., Kubes P. *et al.*, *Phys. Scr.*, **123** (2006) 66.
[12] Soto L., Pavez C., Moreno J. *et al.*, *Phys. Plasmas*, **21** (2014) 122703.
[13] Lerner E., *Laser Part. Beams*, **4** (1986) 193.
[14] Pouzo J. and Milanese M., *IEEE Trans. Plasma Sci.*, **31** (2003) 1237.
[15] Mourenas D., Vierne J., Simonet F. *et al.*, *Phys. Plasmas*, **10** (2003) 605.
[16] Krauz V., Myalton V., Vinogradov V. *et al.*, *Phys. Scr.*, **T161** (2014) 014036.
[17] Krauz V. I., Ananyev S. S., Dan'ko S. A. *et al.*, in *42nd EPS Conference on Plasma Physics, Lisbon, Portugal, 2015*, edited by Bingham R., Suttrop W., Atzeni S., Foest R. and McClements K., Vol. **39E** (EPS) 2015, `http://ocs.ciemat.es/EPS2015PAP/pdf/P4.401.pdf`.
[18] Pavez C., Pedreros J., Tarifeno-Saldivia A. and Soto L., *Phys. Plasmas*, **22** (2015) 040705.
[19] Mitrofanov K. N., Kharrasov A. M., Krauz V. I. *et al.*, *Astron. Rep.*, **61** (2017) 138.
[20] Krauz V. I., Ananyev S. S., Dan'ko S. A. *et al.*, *J. Phys.: Conf. Ser.*, **907** (2017) 012026.
[21] Skladnik-Sadowska E., Dan'ko S. A., Kharrasov A. M. *et al.*, *Phys. Plasmas*, **23** (2016) 122902.
[22] Beskin V. S., Istomin Ya. N., Kharrasov A. M. *et al.*, *Radiophys. Quantum Electron.*, **59** (2017) 900.
[23] Krauz V. I., Beskin V. S. and Velikhov E. P., *Int. J. Mod. Phys. D*, **27** (2018) 1844009.
[24] Kalashnikov I., Chardonnet P., Chechetkin V., Dodin A. and Krauz V. I., *Phys. Plasmas*, **25** (2018) 062901.
[25] Voitenko D. A., Ananyev S. S., Astapenko G. I. *et al.*, *Plasma Phys. Rep.*, **43** (2017) 1132.
[26] Kubes P., Cikhardt J., Cikhardtova B. *et al.*, *Phys. Plasmas*, **24** (2017) 032706.
[27] Mather J. W., *Phys. Fluids*, **8** (1965) 366.
[28] Beskin V. S., Chernoglazov A. V., Kiselev A. M. and Nokhrina E. E., *Mon. Not. R. Acad. Sci.*, **472** (2017) 3971.
[29] Skladnik-Sadowska E., Dan'ko S. A., Kharrasov A. M. *et al.*, *Phys. Plasmas*, **25** (2018) 082715.
[30] Mitrofanov K. N., Krauz V. I., Myalton V. V. *et al.*, *JETP*, **119** (2014) 910.
[31] Krauz V. I., Astapenko G. I., Markoliya A. I. *et al.*, *Astron. Rep.*, **63** (2019) 146.
[32] Reipurth B., Bally J., Hartigan P., Heathcote S. and Morse J., *Astron. J.*, **123** (2002) 362.
[33] Kubes P., Krauz V., Mitrofanov K. *et al.*, *Plasma Phys. Control. Fusion*, **54** (2012) 105023.
[34] Kubes P., Klir D., Kravarik J. *et al.*, *Plasma Phys. Control. Fusion*, **55** (2013) 035011.
[35] Kubes P., Paduch M., Cikhardtova B. *et al.*, *Phys. Plasmas*, **23** (2016) 082704.
[36] Kubes P., Paduch M., Sadowski M. J. *et al.*, *IEEE Trans. Plasma Sci.*, **47** (2019) 339.
[37] Baronova E. O., Krauz V. I., Myalton V. V. *et al.*, *Plasma Phys. Rep.*, **37** (2011) 935.
[38] Beskin V. S., *MHD Flows in Compact Astrophysical Objects* (Springer, Heidelberg) 2010.